

# Electromagnetic $|G_E/G_M|$ ratios of hyperons at large timelike $q^2$

G. Ramalho<sup>1</sup>, M. T. Peña<sup>2,3</sup>, K. Tsushima<sup>4</sup> and Myung-Ki Cheoun<sup>1</sup>

<sup>1</sup>*Department of Physics and OMEG Institute, Soongsil University,  
Seoul 06978, Republic of Korea*

<sup>2</sup>*LIP, Laboratório de Instrumentação e Física Experimental de Partículas,  
Avenida Professor Gama Pinto, 1649-003 Lisboa, Portugal*

<sup>3</sup>*Departamento de Física e Departamento de Engenharia e Ciências Nucleares,  
Instituto Superior Técnico (IST), Universidade de Lisboa, Avenida Rovisco Pais, 1049-001 Lisboa, Portugal*

<sup>4</sup>*Laboratório de Física Teórica e Computacional – LFTC, Universidade Cidade de São Paulo, 01506-000, São Paulo, SP, Brazil*

---

## Abstract

In recent years, it has become possible to measure not only the magnitude of the electric ( $G_E$ ) and magnetic ( $G_M$ ) form factors of spin  $\frac{1}{2}$  baryons, but also to measure the relative phases of those quantities in the timelike kinematic region. Aiming to interpret present  $|G_E/G_M|$  data on hyperons of the baryon octet, as well as to predict future data, we present model calculations of that ratio for large invariant 4-momentum square  $q^2$  in the timelike region ( $q^2 > 0$ ). Without any further parameter fitting, we extend to the timelike region a covariant quark model previously developed to describe the kinematic spacelike region ( $q^2 \leq 0$ ) of the baryon octet form factors. The model takes into account both the effects of valence quarks and the excitations of the meson cloud which dresses the baryons. This application to the timelike region assumes an approximation based on unitarity and analyticity that is valid only in the large  $q^2$  region. Using the recent data from BESIII we establish the regime of validity of this approximation. We report here that our results for the effective form factor (combination of  $|G_E|$  and  $|G_M|$ ) are in good agreement with the data already for  $q^2$  values above 15 GeV<sup>2</sup>. In addition, a more conservative onset of the validity of the approximation is provided by the newly available  $|G_E/G_M|$  data which suggest that our predictions may be compared against data for  $q^2 \geq 20$  GeV<sup>2</sup>. This is expected in the near future, when the range of the present measurements is expanded to the 20–50 GeV<sup>2</sup> region.

---

## 1. Introduction

In recent years it became possible to experimentally probe the structure of short-lived baryons through  $e^+e^- \rightarrow B\bar{B}$  and  $p\bar{p} \rightarrow B\bar{B}$  experiments in the timelike kinematic region above the production threshold  $q^2 \geq 4M_B^2$  ( $M_B$  is the mass of the baryon) [1, 2, 3, 4, 5, 6]. These timelike studies complement the two last decades knowledge on the spacelike region<sup>1</sup> ( $q^2 \leq 0$ ) based on results from electron scattering experiments [7, 8, 9].

The electromagnetic structure of the baryons is represented by spin ( $J$ ) and parity ( $P$ ) dependent structure form factors. In the timelike region these form factors are complex functions of the  $e^+e^-$  or  $p\bar{p}$  square center-of-mass energy  $s = q^2$  [9, 10, 11, 12, 13, 14, 15]. Of

particular interest are the spin  $\frac{1}{2}$  baryons ( $J^P = \frac{1}{2}^\pm$ ), including the nucleon and hyperons characterized by two form factors only, the electric and magnetic form factors. We focus here on hyperons because the experimental information about the nucleon is at the moment less complete. Also, our model uncertainty decreases with increasing  $q^2$ , and the convergence of the nucleon data to the asymptotic large  $q^2$  behavior is expected to emerge at much larger  $q^2$  values, due the dominance of light quark dynamics.

Given the short lifetime of hyperons, the challenges in the determination of their electromagnetic properties in the timelike region, where their weak decays can be analyzed in detail [2] are less significant than in the spacelike region.

The first experiments measured the total integrated cross section of the  $e^+e^- \rightarrow B\bar{B}$  reactions for spin  $\frac{1}{2}$  baryons, which determine the magnitude of the "effec-

---

<sup>1</sup>In this work, for simplicity, we include into the spacelike region the photon point  $q^2 = 0$ , due to the physical continuity between the regions  $q^2 < 0$  and  $q^2 = 0$ .

tive" form factor  $G$  defined as [2, 6]

$$|G(q^2)|^2 = \frac{2\tau|G_M(q^2)|^2 + |G_E(q^2)|^2}{2\tau + 1}, \quad (1)$$

where  $\tau = \frac{q^2}{4M_B^2}$ .

These experiments provided information only about a combination of the electric and magnetic form factors, and did not reveal their relative phases. The separate determination of  $|G_E|$  and  $|G_M|$  or of the ratio  $|G_E/G_M|$  for spin  $\frac{1}{2}$  baryons in the timelike region can be obtained by further measuring the differential cross section [4, 5, 16], while the knowledge of the relative phase between the two form factors demands in addition the determination of polarization cross sections (which involve complete spin separation) [2, 4, 5]. Today, indeed it is possible to measure the ratio  $|G_E/G_M|$  and the relative angle between the form factors for a few baryons [4, 5, 17]. Most measurements to date have been done for ground state hyperons, but in the future excited states may be accessed. In a first experimental period the proton and the neutron form factors were extracted under some assumptions about the relation between  $G_E$  and  $G_M$  [10, 11, 17].

Although the initial measurements were performed near the threshold, it is expected that with increased accelerator power, the experimental energy will go higher up to the 20–50 GeV<sup>2</sup> range. This extension will allow us to test the predictions described in this work.

Measurements of the effective elastic form factors of the  $\Lambda$ ,  $\Sigma^{0,\pm}$ ,  $\Xi^{0,-}$  as well as the transition form factors  $\Sigma^0 \rightarrow \Lambda$  have been performed at BaBar [17], CLEO [3, 18], Belle [19] and BESIII [4, 5, 16, 20, 21, 22, 23, 24, 25, 26, 27, 28, 29, 30, 31]. Measurements of the ratios  $|G_E/G_M|$  for the  $\Lambda$  and  $\Sigma^+$  have also been determined recently at BESIII [4, 5, 16]. Complete experiments, that measure  $|G_E|$ ,  $|G_M|$ , and the relative phase between  $G_E$  and  $G_M$  have been performed for the  $\Lambda$  and  $\Sigma^+$  at BESIII [4, 5], and even more measurements are planned for a near future at BESIII and PANDA [32, 33].

In this work, we enlarge a previous theoretical study of the effective form factors of  $J^P = \frac{1}{2}^+$  hyperons [6] to calculate the  $|G_E/G_M|$  ratios for large  $q^2$ . Calculations in this momentum transfer region are important, given that at very large  $q^2$ ,  $|G_M(q^2)|$  dominates the effective form factor  $|G(q^2)|$ , allowing us to probe where that regime sets in.

The numerical calculations are based on the covariant spectator quark model formalism for the spacelike region [7, 34, 35, 36] extended to the timelike region using asymptotic relations valid for large  $q^2$  [6]. The model has been used in the study of electromagnetic

structure of nucleon resonances [36, 37, 38, 39, 40, 41] and other baryons systems [42, 43, 44].

In the case of the nucleon it is possible to compare the magnitude of  $G_E/G_M$  in the spacelike and timelike regions [13, 34, 44, 45, 46, 47]. Timelike data on the nucleon electromagnetic form factors can be found in Refs. [1, 48, 49, 50, 51, 52] for the proton and in Refs. [15, 53, 54, 55, 56] for the neutron. Theoretical studies of the nucleon electromagnetic form factors in the timelike region can be found in Refs. [57, 58, 59, 60, 61, 62, 63, 64, 65]. At the moment the measurements of the nucleon form factors in the timelike region are incomplete, since their relative phases have not been measured. The data of the proton and neutron effective form factors revealed an oscillatory dependence on the center-of-mass energy [2, 49, 53, 62, 63]. Different explanations have been proposed [57, 59, 64, 66]. In the present work we do not discuss this subject because we are focused on the asymptotic region, where the oscillatory component is expected to be suppressed.

Beyond the members of the baryon octet, there are also measurements of the effective form factors of the  $\Omega^-$ ,  $\Delta$  and  $\Lambda_c^+$  [3, 18, 67, 68, 69]. Theoretical works on hyperon form factors in the timelike region can be found in Refs. [66, 70, 71, 72, 73, 74, 75, 76, 77, 78, 79, 80].

## 2. Formalism

Within the one-photon-exchange approximation, [1, 2] we can write the  $e^+e^- \rightarrow B\bar{B}$  differential cross section, where  $B$  stands for a spin  $\frac{1}{2}$  baryon  $B\left(\frac{1}{2}^\pm\right)$ , as

$$\frac{d\sigma_{\text{Born}}}{d\Omega}(q^2) = \frac{\alpha^2\beta C}{4q^2} \left[ |G_M(q^2)|^2(1 + \cos^2\theta) + \frac{1}{\tau}|G_E(q^2)|^2 \sin^2\theta \right], \quad (2)$$

where  $\theta$  is the angle between the baryon and the initial photon in the center-of-mass frame,  $\alpha \simeq 1/137$  is the fine structure constant,  $\beta = \sqrt{1 - \frac{4M_B^2}{q^2}}$  is a kinematic factor (the baryon speed in  $c = 1$  units) and  $C$  is the Sommerfeld-Gamow factor. This factor takes into account the Coulomb interaction and can be written as  $C = \frac{y}{1 - \exp(-y)}$  with  $y = \frac{\pi\alpha}{\beta} \frac{2M_B}{\sqrt{q^2}}$  for charged particles, and  $C = 1$  for neutral particles [10, 51]. For charged particles the factor  $C$  converges rapidly to  $C \simeq 1$  when  $q^2$  increases.

By integrating the previous relation, we obtain

$$\sigma_{\text{Born}}(q^2) = \frac{4\pi\alpha^2\beta C}{3q^2} \left( 1 + \frac{1}{2\tau} \right) |G(q^2)|^2, \quad (3)$$

using Eq. (1). We can conclude then that the effective form factor can be calculated directly from the integrated cross section. However, it does not give individual information on  $G_E$  or  $G_M$ .

To untangle information on the two form factors  $G_E$  and  $G_M$  one uses the differential cross section (2) by determining the coefficients of the angular functions  $1 + \cos^2 \theta$  and  $\sin^2 \theta$  [1, 2, 24, 30]. Combining the two results, one can extract the ratio  $|G_E/G_M|$ . The measurement of the phase between the form factors requires in addition the measurement of cross section with defined polarizations of the baryons [30].

Finally, at threshold, where  $q^2 = 4M_B^2$ , the functions  $G_E$  and  $G_M$  are such that  $G_E = G_M$ , as a consequence of the definition of these Sachs form factors in terms of the kinematic independent Dirac and Pauli form factors. Therefore one expects that  $G_E/G_M \approx 1$  for measurements near the threshold, and the non-zero phases between the form factors are to be sought above the threshold only ( $q^2 > 4M_B^2$ ) [2].

The main conclusion of this section is that in the case of a spin  $\frac{1}{2}$  baryon, to obtain the absolute values of the two form factors from experiments of the differential cross section it is necessary to measure accurately angular distributions of the differential cross section besides the effective form factor  $|G(q^2)|$ . However, as we will see in the next section the range for non-zero imaginary parts cannot extend to indefinitely large  $|q^2|$ .

### 3. Calculation of electromagnetic form factors at large $q^2$

In this work the electromagnetic form factors  $G_E$  and  $G_M$  in the timelike region are obtained from extrapolating the results from the region  $q^2 = -Q^2 \leq 0$  to the region  $q^2 > 0$ .

For that purpose we consider the large- $|q^2|$  relations

$$G_\ell(q^2) = G_\ell(-q^2) \quad (4)$$

for  $\ell = E, M$ . These asymptotic relations are a consequence of two general mathematical principles: unitarity as well as the Phragmén-Lindelöf theorem, which is valid for analytic functions [10].

We notice that this theorem implies that the imaginary parts of the form factors in the timelike region must be negligible for large  $q^2$ , since the form factors are real in the spacelike region.

The relations (4) are strictly valid in the mathematical limit  $q^2 \rightarrow +\infty$ . Alone the relations provide no information on the range where approximated results can be expected to have a certain accuracy. But the large physical  $q^2$  scale where the mathematical theorem starts to

be valid can be determined by the comparison with the physical data, which we do here.

Given the character of approximation, based on asymptotic relations, we expect our estimates here to be accurate only for large  $q^2$ , deviating from the condition  $G_E = G_M$  at the threshold.

Since the relations (4) are valid for the large- $|q^2|$ , and we want to make predictions for finite  $q^2$ , we consider corrections to these asymptotic relations. We start by noticing that the elastic form factors are divided into two regions of  $q^2$ :  $(-\infty, 0]$  (spacelike region) and  $[4M_B^2, +\infty)$ , with a gap of  $4M_B^2$  length between the photon point ( $q^2 = 0$ ) and the threshold of the baryon-antibaryon production ( $q^2 = 4M_B^2$ ). The interval  $(0, 4M_B^2)$  defines an unphysical region where no physical baryons can be detected [10, 11], but where the peak structure in the form factors can be inferred from the  $e^+e^- \rightarrow \pi^+\pi^-$  cross sections. Only for much larger values of  $q^2$  above the threshold ( $q^2 = 4M_B^2$ ), we expect that the tail of the form factors becomes symmetric to the smooth one of the spacelike region ( $q^2 \leq 0$ ).

It is then clear that  $q^2 = 0$  is not the center of reflection of the asymptotic symmetry relation (4). But there is an ambiguity about the exact location of this center, and to take into account this ambiguity we replace  $q^2 \rightarrow q^2 \left(1 - \frac{2M_B^2}{q^2}\right)$  in (4), which introduces finite corrections ( $-2M_B^2$ ) to the limit  $q^2 = +\infty$ . Therefore we use [6]

$$G_\ell(q^2) = G_\ell^{\text{SL}}(q^2 - 2M_B^2) \quad (5)$$

for  $\ell = E, M$ . The label SL on the r.h.s. indicates that the  $G_\ell^{\text{SL}}(Q^2)$  is calculated in the spacelike region ( $Q^2 = -q^2 \geq 0$ ). The expression (5) estimates the reflection symmetry point underlying (4) exactly at the center of the unphysical interval  $(0, 4M_B^2)$ .

In summary, the measured form factors in the timelike region are complex functions characterized by their magnitudes,  $|G_E|$ ,  $|G_M|$ , and their different phases. Our model calculation is based on results obtained in the  $q^2 \leq 0$  region and the application of the large- $q^2$  relation (5). This way, by construction, we obtain real numbers for  $G_E$  and  $G_M$  that carry  $\pm$  signs. In principle, for very large  $q^2$  the comparison of our results with the experimental values for  $G_E/G_M$  is possible since in that region the relative phase can only have two possibilities,  $\Delta\Phi = 0$  (when the form factors have the same sign) or  $\Delta\Phi = \pi$  (if they have different signs).

For a control of the approximation we explored the band of variation of the form factors with respect to a reasonable variation of the symmetry point around this central value: when the functions  $G_\ell(q^2)$  are positive

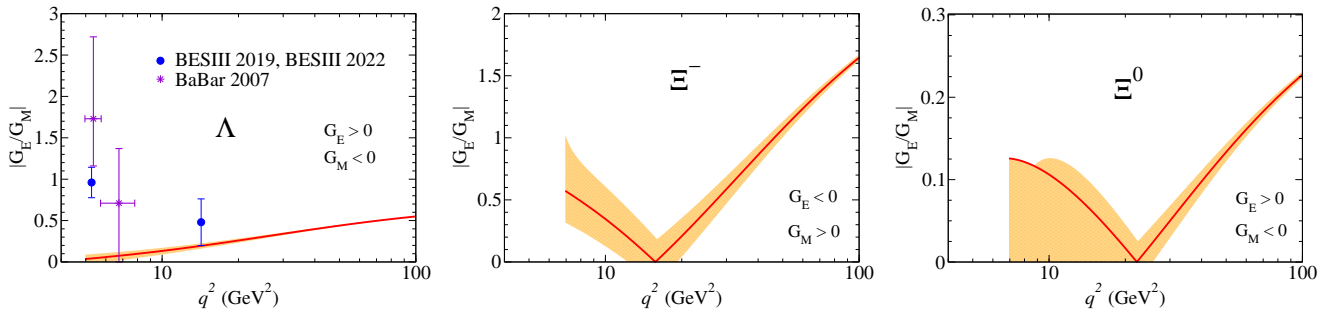


Figure 1: Ratios  $|G_E/G_M|$  for  $\Lambda$ ,  $\Xi^0$  and  $\Xi^-$ . The data for  $\Lambda$  are from BaBar [17] and BESIII [4, 16].

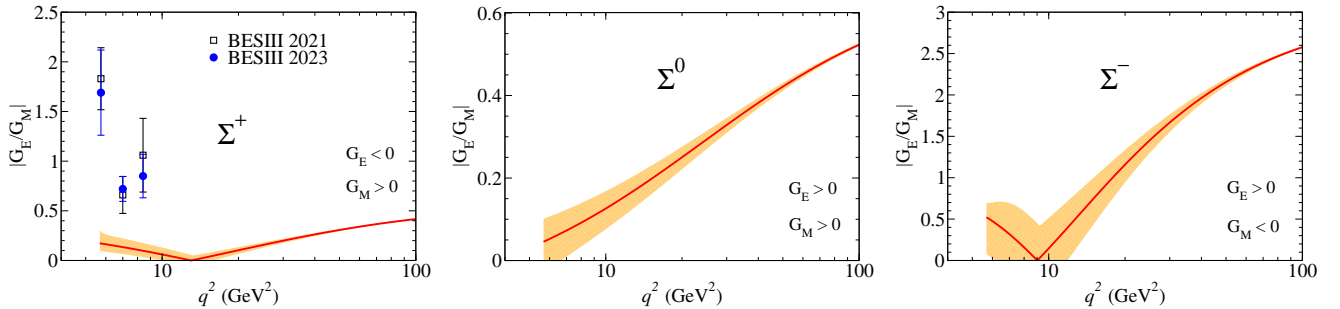


Figure 2: Ratios  $|G_E/G_M|$  for  $\Sigma^+$ ,  $\Sigma^0$  and  $\Sigma^-$ . The data for the  $\Sigma^+$  are from BESIII [5, 24].

(negative), since they are expected to monotonically decrease (increase) with increasing  $q^2$ , we take the upper (lower) limit values to be  $G_\ell(q^2) = G_\ell^{\text{SL}}(q^2 - 4M_B^2)$  and the lower (upper) limit  $G_\ell(q^2) = G_\ell^{\text{SL}}(q^2)$ . This procedure provides a band of variation of the finite corrections to the asymptotic symmetry identity. When  $q^2$  is very large, the variation of the results becomes very narrow and the three estimates (central, upper and lower limits) converge to the same value, providing accurate predictions that can be tested by experimental data.

The relations (5) are naturally valid in the perturbative QCD (pQCD) region, where the form factors are regulated by power laws [81, 82]. Is it possible, however, that they start to be observed earlier than the pQCD regime. The origin of the symmetry relations is unitarity and analyticity. To begin with, the hadron bound states and decays of the hadrons on meson-baryon states seen as peaked structures of the timelike form factors are limited to the confinement region (lower energy). The comparison with data provides information on the onset of the regime of the asymptotic reflection symmetry (4). This is further discussed in Section 5 on the effective form factors.

#### 4. Numerical results for $|G_E/G_M|$

In this section we present our results of the ratio  $|G_E/G_M|$  for large  $q^2$  values. The calculation method of the form factors  $G_E$  and  $G_M$  for the baryon octet family in the timelike region is discussed in detail in Ref. [6] which uses the covariant spectator quark model formalism for the spacelike region [7, 34, 35, 36]. In its nutshell, we use impulse approximation for the electromagnetic quark current, which is justified for large  $Q^2$ , since then the interacting photon has sufficient resolution to interact with a single quark at a time. As a result we can integrate over the relative internal variables of the spectator quarks and therefore we end up with the baryon three-quark system regarded as a quark-diquark configuration. In the model, the SU(3) symmetry quark flavor symmetry is broken at the level of the baryon radial wave functions and the constituent quark current [35, 43, 83], and gluon and quark-antiquark dressing are effectively taken into the constituent quark structure.

The different baryon radial wave functions are parametrized by two parameters, a short range scale and a long range scale, consistent with the expected size of the systems (baryons with strange quarks are more com-

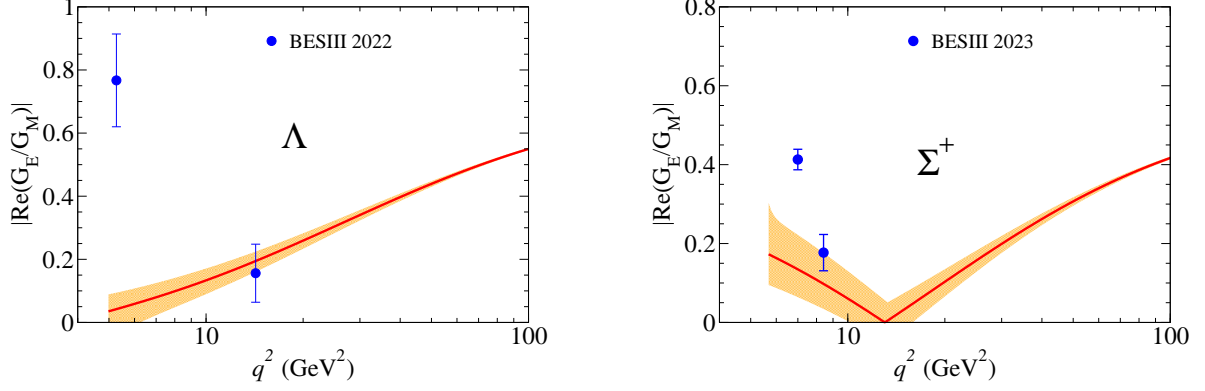


Figure 3: Model calculations of  $|G_E/G_M|$  for  $\Lambda$  and  $\Sigma^+$  compared with the  $|\text{Re}(G_E/G_M)|$  data from BESIII for  $\Lambda$  [16] and  $\Sigma^+$  [5].

fact than baryons with light quarks) [43]. The quark current is parametrized by vector meson dominance regulated by light ( $\rho$ ,  $\omega$ ) and intermediate ( $\phi$ ) vector meson mass poles [35, 43].

In particular, we use the parameterization of the baryon octet from Refs. [43]. To the valence quark contributions we add also an effective description of meson cloud dressing processes [41, 83, 84, 85, 86], which are inevitably present in the low- $Q^2$  region. In the large- $|Q^2|$  region, the meson cloud contributions are suppressed and their effects are manifest on the rescaling of the bare contributions to the form factors due to the normalization of the hyperon wave functions [6, 43]. This formalism has been used to successfully describe the spacelike electromagnetic structure data of baryons including the low-lying nucleon resonances [9, 36]. The free parameters of the model are fixed by the data for the nucleon, baryon octet and baryon decuplet [34, 43, 44, 83, 85, 86].

Our calculations of the ratio  $|G_E/G_M|$  and their comparison with the data are shown in Figs. 1 and 2, that depict the results for  $\Lambda$ ,  $\Xi^{-,0}$  and the  $\Sigma^{0,\pm}$ , respectively. In the graphs for the  $\Lambda$  and  $\Sigma^+$  we include the available data for  $|G_E/G_M|$ . How we estimate the uncertainty of the results of our model for each form factor was defined in the previous section. The bands of variation for the magnitude of  $G_E/G_M$  are determined from the independent band intervals of variation for the  $G_E$  and  $G_M$  functions.

The results and their uncertainty bands near the threshold provide only qualitative estimates since our results are expected to be valid only for large  $q^2$ , as discussed in the previous section. The deviation from the result  $|G_E/G_M| = 1$  at threshold is a consequence of the approximation used. The signs of our results for the form factors in the asymptotic large  $q^2$  values are indi-

cated on the right side in Figs. 1 and 2.

The separated calculations of the form factors  $G_E$  and  $G_M$  for  $\Lambda$ ,  $\Sigma^{0,\pm}$  and  $\Xi^{-,0}$  are presented in the Supplementary Material [87].

Note that we are not attempting to predict the zeros of  $G_E/G_M$ , rather, we are focused on determining its magnitude at sufficiently large  $q^2$ . In the current formalism, the zeros can only be determined within an uncertainty band of width  $4M_B^2$  for  $q^2$ .

We discuss now how we can take into account the information of the relative angle between the form factors in the analysis of the ratio  $|G_E/G_M|$ . In complete experiments the ratio  $G_E/G_M$  is determined, and can be written in the form

$$\frac{G_E}{G_M} = \frac{|G_E|}{|G_M|} e^{i\Delta\Phi}, \quad (6)$$

where  $|G_\ell|$  is the magnitude of the complex form factor  $G_\ell$  and  $\Delta\Phi$  is the phase between  $G_E$  and  $G_M$ . Once the phase is measured, we can extract the real part of the ratio from

$$\left| \text{Re} \left( \frac{G_E}{G_M} \right) \right| = \left| \frac{G_E}{G_M} \right| |\cos(\Delta\Phi)|, \quad (7)$$

which is a fraction of the measured value to  $|G_E/G_M|$ . This does not only show that model calculations of  $|G_E/G_M|$  based on real form factors agree with the absolute value of the real part of  $G_E/G_M$  when the imaginary parts are negligible. The result (7) allows also us to infer from the comparison between the experimental data for the r.h.s. and our model results for the ratio  $\frac{|G_E|}{|G_M|}$  (where  $G_E$  and  $G_M$  are real functions) if the regime where the imaginary parts of the form factors vanish has been attained. The comparison of our model results for  $|G_E/G_M|$  with the experimental values for  $|\text{Re}(G_E/G_M)|$  from Refs. [16, 31] that measure phases, are displayed

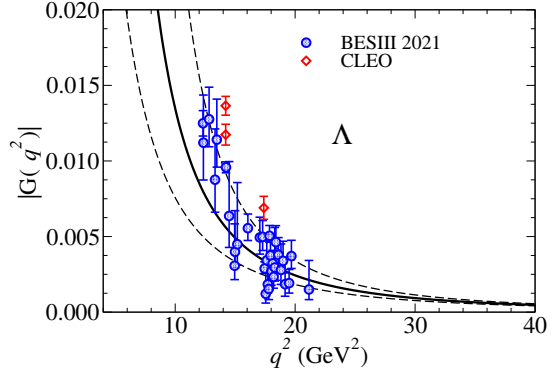
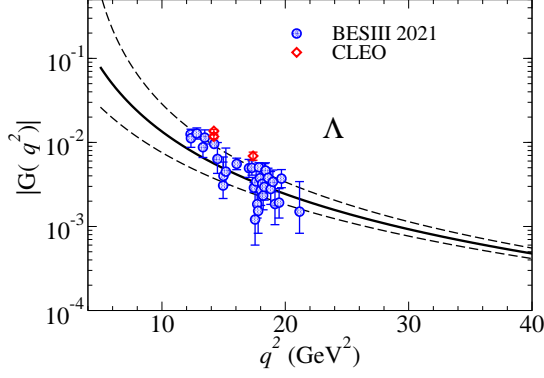


Figure 4: Effective form factor  $|G(q^2)|$  for  $\Lambda$ . The data are from BaBar [17], CLEO [3, 18] and BESIII 2021 [21].

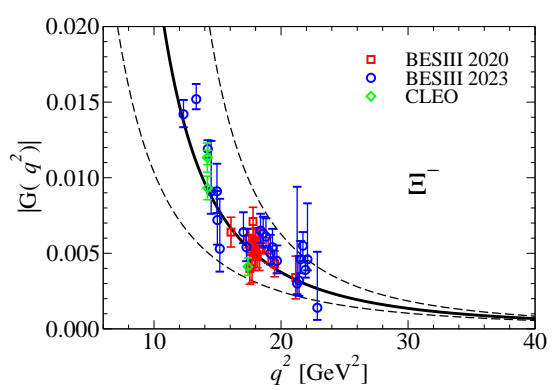
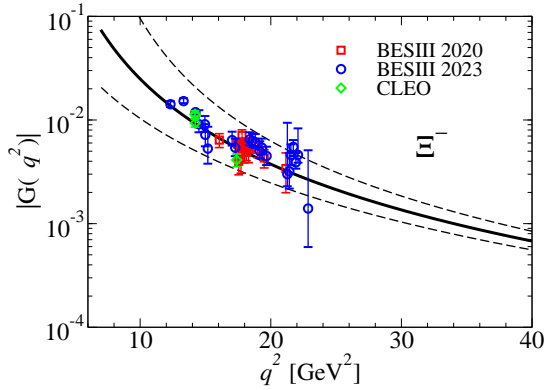


Figure 5: Effective form factor  $|G(q^2)|$  for  $\Xi^-$ . The data are from CLEO [3], BESIII 2020 [29] and BESIII 2023 [30].

in Fig. 3. In the graphs we notice the agreement of our results for the form factors (considering the model uncertainty band) and the experimental data point at the largest  $q^2$  point measured,  $q^2 \simeq 14.3 \text{ GeV}^2$  for the  $\Lambda$  and  $q^2 \simeq 8.4 \text{ GeV}^2$  for the  $\Sigma^+$ . In the graphs we ignore the uncertainties of the angles  $\Delta\Phi$ , for simplicity, and used their central value. The consideration of the uncertainties on  $\Delta\Phi$  only increases the error bars of the  $|\text{Re}(G_E/G_M)|$  data.

It is worth noticing that the agreement between model calculations and the data is not an indication that we are in the pQCD regime. Evidences of scaling with the pQCD behavior for the nucleon are observed only for  $Q^2 \geq 30 \text{ GeV}^2$  [82]. One expects, however, that the convergence for the pQCD regime can be seen for lower values of  $q^2$  for hyperons due to dynamics of the strange quarks.

Future experiments with more precise data can help to determine the point where our model calculations provide a good description of the data and determine the  $q^2$  region where reflection symmetry sets in.

## 5. Effective form factors

In a previous work [6] we presented predictions for the effective form factors (1) for the baryon octet members  $\Lambda$ ,  $\Sigma^{0,\pm}$  and  $\Xi^{0,-}$  for  $q^2 = 10\text{--}60 \text{ GeV}^2$ . At the time, only  $\Lambda$ ,  $\Sigma^+$ ,  $\Sigma^-$ ,  $\Xi^0$  and  $\Xi^-$  could be tested in the region of  $12\text{--}15 \text{ GeV}^2$  by the data from CLEO [3]. Our estimates were on average consistent with the high  $q^2$  data. Since then more data for  $|G(q^2)|$  became available. In particular data for  $\Sigma^+$  and  $\Sigma^-$  became available from BESIII [28] for the range  $5.7\text{--}9.1 \text{ GeV}^2$ . Surprisingly, the data are in excellent agreement with our estimates (namely with the central line values, see Supplementary Material [87]) even outside the region where model validity was expected to be justified. A rough estimate of the lower limit for the application of our model based on the asymptotic relations, can be  $q^2 \approx 10 \text{ GeV}^2$  or  $q^2 \approx 8M_B^2$ .

Recently, data from BESIII became available for  $\Lambda$  up to  $q^2 = 21 \text{ GeV}^2$  [21], and for  $\Xi^-$  up to  $q^2 = 23 \text{ GeV}^2$  [5, 24]. The new data are compatible with the CLEO data and extend the previous range covered by

the experiments. The comparison of the new data with the model results from Ref. [6] is presented in Figs. 4 and 5 in a linear scale and in the logarithm scale for  $|G(q^2)|$ .

It is clear from the figures that there is an excellent agreement between our predictions and the data for  $q^2 > 15 \text{ GeV}^2$ , indicating that we are already in the range of the asymptotic form for the effective form factors. Compared to the convergence to the pQCD regime, a faster convergence of the reflection symmetry relations to their asymptotic behavior can be expected because in the effective form factors  $G_M$  dominates on  $|G|$  for large  $q^2$ : for instance, for the case of the nucleon,  $G_M$  dominates over  $G_E$ , and  $G_M$  converges to the expected power law faster than  $G_E$ , in the spacelike region [34, 44].

Future data may confirm or deny if we are also close to the range of the asymptotic region for the ratio  $|G_E/G_M|$ .

Calculations of the effective form factors for all the hyperons of the baryon octet are presented in Supplementary Material [87] and compared with the world data.

## 6. Outlook and conclusions

Experiments in new facilities (BaBar, CLEO, Belle, PANDA etc.) allow us to access the electromagnetic structure of hyperons in the elastic timelike region ( $q^2 \geq 4M_B^2$ ). Till recently we had access only to the integrated cross section which can be used to determine the effective form factor  $|G|$ , and encode only the information of a certain combination of the electric and magnetic form factors  $|G_E|$  and  $|G_M|$ , for spin  $\frac{1}{2}$  hyperons. No separated information about  $|G_E|$  and  $|G_M|$  was possible till a few years ago. Even the separation between  $|G_E|$  and  $|G_M|$  for the proton and neutron was difficult and affected by significant errors.

In the last few years it became possible to determine  $|G_E|$  and  $|G_M|$  and the relative phase between them for  $\Lambda$  and  $\Sigma^+$ . We expect that the ratio  $|G_E/G_M|$  became accessible in the following years for most ground state hyperons ( $\Sigma^{0,-}$  and  $\Xi^{0,-}$ ), as well as for charmed baryons (starting with  $\Lambda_c^+$ ). Our calculations show the start of a partial agreement with the data for  $q^2 \simeq 14 \text{ GeV}^2$  ( $\sqrt{s} \simeq 3.8 \text{ GeV}$ ), which may be an indication that our model calculations may be compared with future measurements in the range of  $q^2 = 20\text{--}30 \text{ GeV}^2$  ( $\sqrt{s} = 4.5\text{--}5.5 \text{ GeV}$ ) or higher. Also the separation between the real and imaginary components may be tested in that range of energies.

## Acknowledgments

G.R. was supported the Basic Science Research Program through the National Research Foundation of Korea (NRF) funded by the Ministry of Education (Grant No. NRF-2021R1A6A1A03043957). M.T.P. was supported by the Portuguese Science Foundation FCT under project CERN/FIS-PAR/0023/2021, and FCT computing project 2021.09667. K.T. was supported by Conselho Nacional de Desenvolvimento Científico e Tecnológico (CNPq, Brazil), Processes No. 313063/2018-4 and No. 426150/2018-0, and FAPESP Process No. 2019/00763-0 and No. 2023/07313-6, and his work was also part of the projects, Instituto Nacional de Ciência e Tecnologia - Nuclear Physics and Applications (INCT-FNA), Brazil, Process No. 464898/2014-5. The work of M.K.C. was supported by the National Research Foundation of Korea (Grant Nos. NRF-2021R1A6A1A03043957 and NRF-2020R1A2C3006177).

## References

- [1] M. Ablikim *et al.* [BESIII], Phys. Rev. D **91** (2015) 112004 [arXiv:1504.02680 [hep-ex]].
- [2] M. Ablikim *et al.* [BESIII], Chin. Phys. C **44** (2020) 040001 [arXiv:1912.05983 [hep-ex]].
- [3] S. Dobbs, K. K. Seth, A. Tomaradze, T. Xiao and G. Bonvicini, Phys. Rev. D **96** (2017) 092004 [arXiv:1708.09377 [hep-ex]].
- [4] M. Ablikim *et al.* [BESIII], Phys. Rev. Lett. **123**, (2019) 122003 [arXiv:1903.09421 [hep-ex]].
- [5] M. Ablikim *et al.* [BESIII], Phys. Rev. Lett. **132** (2024) 081904 [arXiv:2307.15894 [hep-ex]].
- [6] G. Ramalho, M. T. Peña and K. Tsushima, Phys. Rev. D **101** (2020) 014014 [arXiv:1908.04864 [hep-ph]].
- [7] I. G. Aznauryan, A. Bashir, V. Braun, S. J. Brodsky, V. D. Burkert, L. Chang, C. Chen, B. El-Bennich, I. C. Cloet and P. L. Cole, *et al.* Int. J. Mod. Phys. E **22** (2013) 1330015 [arXiv:1212.4891 [nucl-th]].
- [8] I. G. Aznauryan and V. D. Burkert, Prog. Part. Nucl. Phys. **67** (2012) 1 [arXiv:1109.1720 [hep-ph]].
- [9] G. Ramalho and M. T. Peña, Prog. Part. Nucl. Phys. **136** (2024) 104097 [arXiv:2306.13900 [hep-ph]].
- [10] S. Pacetti, R. Baldini Ferroli and E. Tomasi-Gustafsson, Phys. Rept. **550** (2015) 1.
- [11] A. Denig and G. Salme, Prog. Part. Nucl. Phys. **68** (2013) 113 [arXiv:1210.4689 [hep-ex]].
- [12] G. Ramalho, Phys. Rev. D **103** (2021) 074018 [arXiv:2012.11710 [hep-ph]].
- [13] K. K. Seth, S. Dobbs, Z. Metreveli, A. Tomaradze, T. Xiao and G. Bonvicini, Phys. Rev. Lett. **110** (2013) 022002 [arXiv:1210.1596 [hep-ex]].
- [14] N. Cabibbo and R. Gatto, Phys. Rev. **124** (1961) 1577.
- [15] D. Bisello *et al.* [DM2 Collaboration], Z. Phys. C **48** (1990) 23.
- [16] M. Ablikim *et al.* [BESIII], Phys. Rev. D **105** (2022) L011101 [arXiv:2111.11742 [hep-ex]].
- [17] B. Aubert *et al.* [BaBar Collaboration], Phys. Rev. D **76** (2007) 092006 [arXiv:0709.1988 [hep-ex]].
- [18] S. Dobbs, A. Tomaradze, T. Xiao, K. K. Seth and G. Bonvicini, Phys. Lett. B **739** (2014) 90 [arXiv:1410.8356 [hep-ex]].

- [19] G. Gong *et al.* [Belle], Phys. Rev. D **107** (2023) 072008 [arXiv:2210.16761 [hep-ex]].
- [20] M. Ablikim *et al.* [BESIII], Phys. Rev. D **107** (2023) 072005 [arXiv:2303.07629 [hep-ex]].
- [21] M. Ablikim *et al.* [BESIII], Phys. Rev. D **104** (2021) L091104 [arXiv:2108.02410 [hep-ex]].
- [22] M. Ablikim *et al.* [BESIII], JHEP **10** (2023) 081 [arXiv:2303.00271 [hep-ex]].
- [23] M. Ablikim *et al.* [BESIII], Phys. Rev. D **97** (2018) 032013 [arXiv:1709.10236 [hep-ex]].
- [24] M. Ablikim *et al.* [BESIII], Phys. Lett. B **814** (2021) 136110 [arXiv:2009.01404 [hep-ex]].
- [25] M. Ablikim *et al.* [BESIII], JHEP **05** (2024) 022 [arXiv:2401.09468 [hep-ex]].
- [26] M. Ablikim *et al.* [BESIII], Phys. Rev. D **109** (2024) 034029 [arXiv:2312.12719 [hep-ex]].
- [27] M. Ablikim *et al.* [BESIII], Phys. Lett. B **831** (2022) 137187 [arXiv:2110.04510 [hep-ex]].
- [28] M. Ablikim *et al.* [BESIII], Phys. Lett. B **820** (2021) 136557 [arXiv:2105.14657 [hep-ex]].
- [29] M. Ablikim *et al.* [BESIII], Phys. Rev. Lett. **124** (2020) 032002 [arXiv:1910.04921 [hep-ex]].
- [30] M. Ablikim *et al.* [BESIII], JHEP **11** (2023) 228 [arXiv:2309.04215 [hep-ex]].
- [31] M. Ablikim *et al.* [BESIII], Phys. Rev. D **109** (2024) 012002 [arXiv:2308.03361 [hep-ex]].
- [32] B. Singh *et al.* [PANDA], Eur. Phys. J. A **52** (2016) 325 [arXiv:1606.01118 [hep-ex]].
- [33] K. Schönning [PANDA], EPJ Web Conf. **241** (2020) 01015.
- [34] F. Gross, G. Ramalho and M. T. Peña, Phys. Rev. C **77** (2008) 015202 [arXiv:nucl-th/0606029 [nucl-th]].
- [35] G. Ramalho, K. Tsushima and F. Gross, Phys. Rev. D **80** (2009) 033004 [arXiv:0907.1060 [hep-ph]].
- [36] G. Ramalho, Few Body Syst. **59** (2018) 92 [arXiv:1801.01476 [hep-ph]].
- [37] G. Ramalho, M. T. Peña and F. Gross, Phys. Rev. D **78** (2008) 114017 [arXiv:0810.4126 [hep-ph]]; G. Ramalho, Phys. Rev. D **94** (2016) 114001 [arXiv:1606.03042 [hep-ph]]; G. Ramalho, Eur. Phys. J. A **54** (2018) 75 [arXiv:1709.07412 [hep-ph]].
- [38] G. Ramalho and K. Tsushima, Phys. Rev. D **89** (2014) 073010 [arXiv:1402.3234 [hep-ph]]; G. Ramalho and K. Tsushima, Phys. Rev. D **81** (2010) 074020 [arXiv:1002.3386 [hep-ph]].
- [39] G. Ramalho, Phys. Rev. D **90** (2014) 033010 [arXiv:1407.0649 [hep-ph]]; G. Ramalho and M. T. Peña, Phys. Rev. D **101** (2020) 114008 [arXiv:2003.04850 [hep-ph]]; G. Ramalho and M. T. Peña, Phys. Rev. D **84** (2011) 033007. [arXiv:1105.2223 [hep-ph]].
- [40] G. Ramalho, Phys. Rev. D **95** (2017) 054008 [arXiv:1612.09555 [hep-ph]]; G. Ramalho and M. T. Peña, Phys. Rev. D **89** (2014) 094016 [arXiv:1309.0730 [hep-ph]]. G. Ramalho and M. T. Peña, Phys. Rev. D **95** (2017) 014003 [arXiv:1610.08788 [nucl-th]].
- [41] G. Ramalho and M. T. Peña, Phys. Rev. D **80** (2009) 013008 [arXiv:0901.4310 [hep-ph]]; G. Ramalho and M. T. Peña, J. Phys. G **36** (2009) 115011 [arXiv:0812.0187 [hep-ph]].
- [42] G. Ramalho, M. T. Peña and F. Gross, Phys. Rev. D **81** (2010) 113011 [arXiv:1002.4170 [hep-ph]]; G. Ramalho and M. T. Peña, J. Phys. G **36** (2009) 085004 [arXiv:0807.2922 [hep-ph]]; G. Ramalho and M. T. Peña, Phys. Rev. D **83** (2011) 054011 [arXiv:1012.2168 [hep-ph]].
- [43] G. Ramalho and K. Tsushima, Phys. Rev. D **84** (2011) 054014 [arXiv:1107.1791 [hep-ph]]; G. Ramalho and K. Tsushima, Phys. Rev. D **86** (2012) 114030 [arXiv:1210.7465 [hep-ph]].
- [44] G. Ramalho, K. Tsushima and A. W. Thomas, J. Phys. G **40** (2013) 015102 [arXiv:1206.2207 [hep-ph]].
- [45] G. Ramalho, J. P. B. C. de Melo and K. Tsushima, Phys. Rev. D **100** (2019) 014030 [arXiv:1902.08844 [hep-ph]].
- [46] A. J. R. Puckett *et al.*, Phys. Rev. C **96** (2017) 055203 Erratum: [Phys. Rev. C **98** (2018) 019907] [arXiv:1707.08587 [nucl-ex]].
- [47] E. Tomasi-Gustafsson and M. P. Rekalo, Phys. Lett. B **504** (2001) 291.
- [48] M. Ablikim *et al.* [BESIII], Phys. Rev. Lett. **124** (2020) 042001 [arXiv:1905.09001 [hep-ex]].
- [49] M. Ablikim *et al.* [BESIII], Phys. Lett. B **817** (2021) 136328 [arXiv:2102.10337 [hep-ex]]; M. Ablikim *et al.* [BESIII], Phys. Rev. D **99** (2019) 092002 [arXiv:1902.00665 [hep-ex]].
- [50] J. P. Lees *et al.* [BaBar], Phys. Rev. D **87** (2013) 092005 [arXiv:1302.0055 [hep-ex]].
- [51] B. Aubert *et al.* [BaBar Collaboration], Phys. Rev. D **73** (2006) 012005 [arXiv:hep-ex/0604007 [hep-ex]].
- [52] M. Ambrogiani *et al.* [E835 Collaboration], Phys. Rev. D **60** (1999) 032002; T. A. Armstrong *et al.* [E760 Collaboration], Phys. Rev. Lett. **70** (1993) 1212.
- [53] M. Ablikim *et al.* [BESIII], Nature Phys. **17** (2021) 1200 [arXiv:2103.12486 [hep-ex]].
- [54] M. Ablikim *et al.* [BESIII], Phys. Rev. Lett. **130** (2023) 151905 [arXiv:2212.07071 [hep-ex]].
- [55] M. N. Achasov *et al.* [SND], Eur. Phys. J. C **82** (2022) 761 [arXiv:2206.13047 [hep-ex]]; M. N. Achasov *et al.*, Phys. Rev. D **90** (2014) 112007 [arXiv:1410.3188 [hep-ex]].
- [56] A. Antonelli *et al.*, Nucl. Phys. B **517** (1998) 3.
- [57] B. Yan, C. Chen, X. Li and J. J. Xie, Phys. Rev. D **109** (2024) 036033 [arXiv:2312.04866 [nucl-th]].
- [58] Y. H. Lin, H. W. Hammer and U. G. Meißner, Eur. Phys. J. A **57** (2021) 255 [arXiv:2106.06357 [hep-ph]].
- [59] Y. H. Lin, H. W. Hammer and U. G. Meißner, Phys. Rev. Lett. **128** (2022) 052002 [arXiv:2109.12961 [hep-ph]].
- [60] E. A. Kuraev, E. Tomasi-Gustafsson and A. Dbeysi, Phys. Lett. B **712** (2012) 240 [arXiv:1106.1670 [hep-ph]].
- [61] E. Tomasi-Gustafsson, A. Bianconi and S. Pacetti, Phys. Rev. C **103** (2021) 035203 [arXiv:2012.14656 [hep-ph]].
- [62] I. T. Lorenz, H. W. Hammer and U. G. Meißner, Phys. Rev. D **92** (2015) 034018 [arXiv:1506.02282 [hep-ph]].
- [63] A. Bianconi and E. Tomasi-Gustafsson, Phys. Rev. Lett. **114** (2015) 232301 [arXiv:1503.02140 [nucl-th]].
- [64] X. Cao, J. P. Dai and H. Lenske, Phys. Rev. D **105** (2022) L071503 [arXiv:2109.15132 [hep-ph]].
- [65] Q. H. Yang, D. Guo, M. Y. Li, L. Y. Dai, J. Haidenbauer and U. G. Meißner, JHEP **08** (2024) 208 [arXiv:2404.12448 [nucl-th]].
- [66] E. Tomasi-Gustafsson and S. Pacetti, Phys. Rev. C **106** (2022) 035203.
- [67] M. Ablikim *et al.* [BESIII], Phys. Rev. Lett. **120** (2018) 132001 [arXiv:1710.00150 [hep-ex]].
- [68] M. Ablikim *et al.* [BESIII], Phys. Rev. D **108** (2023) 072010 [arXiv:2305.12166 [hep-ex]].
- [69] M. Ablikim *et al.* [BESIII], Phys. Rev. D **107** (2023) 052003 [arXiv:2212.03693 [hep-ex]].
- [70] J. G. Körner and M. Kuroda, Phys. Rev. D **16** (1977) 2165.
- [71] J. Haidenbauer, T. Hippchen, K. Holinde, B. Holzenkamp, V. Mull and J. Speth, Phys. Rev. C **45** (1992) 931.
- [72] J. Haidenbauer and U. G. Meißner, Phys. Lett. B **761** (2016) 456 [arXiv:1608.02766 [nucl-th]].
- [73] Y. H. Lin, H. W. Hammer and U. G. Meißner, Eur. Phys. J. C **82** (2022) 1091 [arXiv:2208.14802 [hep-ph]].
- [74] Y. Yang, D. Y. Chen and Z. Lu, Phys. Rev. D **100** (2019) 073007 [arXiv:1902.01242 [hep-ph]].
- [75] X. Cao, J. P. Dai and Y. P. Xie, Phys. Rev. D **98** (2018) 094006 [arXiv:1808.06382 [hep-ph]].
- [76] A. Mangoni, S. Pacetti and E. Tomasi-Gustafsson, Phys. Rev. D



- 104** (2021) 116016 [arXiv:2109.03759 [hep-ph]].
- [77] A. Bianconi and E. Tomasi-Gustafsson, Phys. Rev. C **105** (2022) 065206 [arXiv:2204.05197 [hep-ph]].
- [78] J. P. Dai, X. Cao and H. Lenske, Phys. Lett. B **846** (2023) 138192 [arXiv:2304.04913 [hep-ph]].
- [79] A. X. Dai, Z. Y. Li, L. Chang and J. J. Xie, Chin. Phys. C **46** (2022) 073104 [arXiv:2112.06264 [hep-ph]].
- [80] Y. M. Bystritskiy and A. I. Ahmadov, Phys. Rev. D **105** (2022) 116012 [arXiv:2204.08956 [hep-ph]].
- [81] S. J. Brodsky and G. R. Farrar, Phys. Rev. D **11** (1975) 1309.
- [82] P. Mergell, U. G. Meißner and D. Drechsel, Nucl. Phys. A **596** (1996) 367 [arXiv:hep-ph/9506375 [hep-ph]].
- [83] G. Ramalho and K. Tsushima, Phys. Rev. D **87** (2013) 093011 [arXiv:1302.6889 [hep-ph]]; G. Ramalho and K. Tsushima, Phys. Rev. D **88** (2013) 053002 [arXiv:1307.6840 [hep-ph]].
- [84] G. Ramalho, M. T. Peña, J. Weil, H. van Hees and U. Mosel, Phys. Rev. D **93** (2016) 033004 [arXiv:1512.03764 [hep-ph]]; G. Ramalho and M. T. Peña, Phys. Rev. D **85** (2012) 113014 [arXiv:1205.2575 [hep-ph]].
- [85] G. Ramalho, Phys. Rev. D **102** (2020) 054016 [arXiv:2002.07280 [hep-ph]]; G. Ramalho and K. Tsushima, Phys. Rev. D **108** (2023) 074019 [arXiv:2308.04773 [hep-ph]].
- [86] G. Ramalho, D. Jido and K. Tsushima, Phys. Rev. D **85** (2012) 093014 [arXiv:1202.2299 [hep-ph]].
- [87] [Supplementary material](#).

# Electromagnetic $|G_E/G_M|$ ratios of hyperons at large timelike $q^2$

## Supplementary Material

We present here calculations of the form factors  $G_E$  and  $G_M$  and the effective form factor  $G$  in the timelike region for the hyperons  $\Lambda$ ,  $\Xi^{-,0}$  and the  $\Sigma^{0,\pm}$ .

### Form factors $G_E$ and $G_M$

The absolute values of the form factors  $G_E$  and  $G_M$  are presented in Fig. S1. The signs of  $G_E$  and  $G_M$  can be inferred from the labels included in the figures. The representation  $-G_E$  or  $-G_M$  indicate that the functions are negative in that region. The cusps indicate the zero of  $G_E$ .

### Effective form factors $G$

The effective form factors are presented in Fig. S2. The limits of the theoretical calculations are represented by the dashed lines.

**Data**  $\Sigma^+$ : Belle [S1], BESIII [S3, S2, S4], and CLEO [S5, S6]; **Data**  $\Sigma^0$ : BaBar [S7], BESIII [S8], CLEO [S5, S6] and Belle [S1]; **Data**  $\Sigma^-$ : BESIII [S3]; **Data**  $\Lambda$ : BaBar [S7], BESIII [S9, S10] and CLEO [S5, S6]; **Data**  $\Xi^0$ : BESIII [S11] and CLEO [S5, S6]; **Data**  $\Xi^-$ : BESIII [S12, S13] and CLEO [S5, S6].

### References

- [S1] G. Gong *et al.* [Belle], Phys. Rev. D **107** (2023) 072008.
- [S2] M. Ablikim *et al.* [BESIII], JHEP **05** (2024) 022.
- [S3] M. Ablikim *et al.* [BESIII], Phys. Lett. B **814** (2021) 136110.
- [S4] M. Ablikim *et al.* [BESIII], Phys. Rev. D **109** (2024) 034029.
- [S5] S. Dobbs, A. Tomaradze, T. Xiao, K. K. Seth and G. Bonvicini, Phys. Lett. B **739** (2014) 90.
- [S6] S. Dobbs, K. K. Seth, A. Tomaradze, T. Xiao and G. Bonvicini, Phys. Rev. D **96** (2017) 092004.
- [S7] B. Aubert *et al.* [BaBar Collaboration], Phys. Rev. D **76** (2007) 092006.
- [S8] M. Ablikim *et al.* [BESIII], Phys. Lett. B **831** (2022) 137187.
- [S9] M. Ablikim *et al.* [BESIII], Phys. Rev. D **104** (2021) L091104.
- [S10] M. Ablikim *et al.* [BESIII], Phys. Rev. D **107** (2023) 072005.
- [S11] M. Ablikim *et al.* [BESIII], Phys. Lett. B **820** (2021) 136557.
- [S12] M. Ablikim *et al.* [BESIII], Phys. Rev. Lett. **124** (2020) 032002.
- [S13] M. Ablikim *et al.* [BESIII], JHEP **11** (2023) 228.

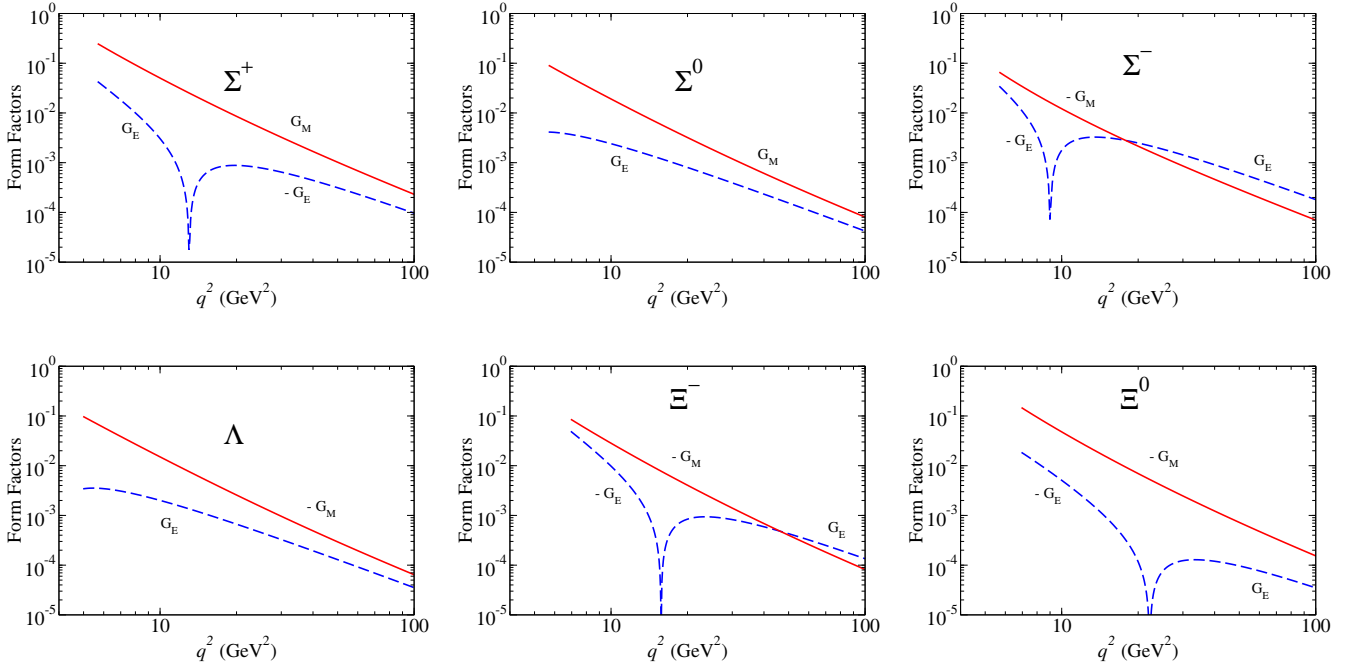


Figure S1: Model calculations of  $G_E$  and  $G_M$ .

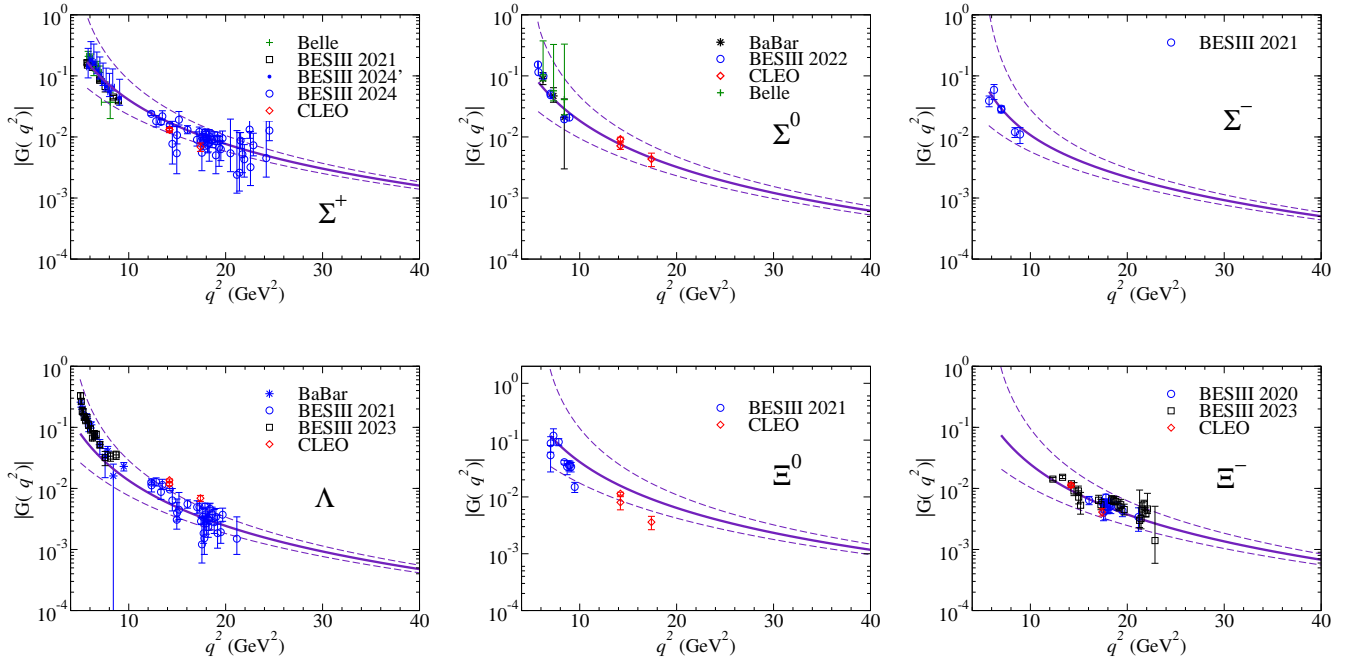


Figure S2: Model calculations of hyperon effective form factors compared with the data.